Ecotoxicology and Environmental Safety 246 (2022) 114181

Contents lists available at ScienceDirect

Ecotoxicology and Environmental Safety

journal homepage: www.elsevier.com/locate/ecoenv

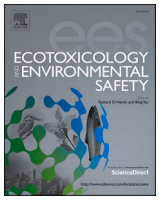

Estrogen deficiency aggravates fluoride-induced small intestinal mucosa damage and junctional complexes proteins expression disorder in rats

Ye Jin, Xiao-ying Gao, Jing Zhao, Wei-shun Tian, Yu-ling Zhang, Er-jie Tian, Bian-hua Zhou, Hong-wei Wang *

Henan Key Laboratory of Environmental and Animal Product Safety, Henan University of Science and Technology, Luoyang 471000, Henan, People's Republic of China

ARTICLE INFO

Edited by Dr. Caterina Faggio

Keywords:
Fluorosis
Intestinal mucosa
Tight junction proteins
Goblet cells
Glycoproteins
Estrogen

ABSTRACT

To investigate the effect of estrogen deficiency on the small intestinal mucosal barrier induced by fluoride (F), F exposure models of ovariectomy (OVX) rats (surgically removed ovaries) and non-OVX rats (normal condition) were established by adding sodium fluoride (NaF) (0, 25, 50, and 100 mg/L, calculated by F ion) in drinking water for 90 days. The intestinal mucosal histomorphology, mucosal barrier function, and protein expression levels of tight junctions (TJs), adhesion junctions (AJs), and desmosomes were evaluated in the duodenum, jejunum, and ileum. Hematoxylin-eosin (HE) staining and 5-Bromo-2-deoxyUridine (BrdU) measurement showed that excessive F-induced damage to intestinal epithelial cells and inhibited the proliferation of intestinal epithelial cells, eventually decreasing the number of goblet cells and decreasing glycoprotein secretion, as indicated by Alcian blue and periodic acid-Schiff (AB-PAS) and periodic acid-Schiff (PAS) staining. Further immunofluorescence analysis demonstrated that excessive F decreased the protein expression levels of occludin, zonula occludens-1 (ZO-1), E-cadherin, and desmoplakin ($P < 0.05$, $P < 0.01$) and enhanced the expression of claudin-2 ($P < 0.01$), suggesting that cell-to-cell junctions were disrupted. Collectively, F exposure impaired the small intestinal mucosal barrier by inducing damage to intestinal epithelial cells and inhibiting intestinal epithelial cell proliferation. Disorders in the junctional complex protein expression blocked the synergy between intercellular communication and aggravated mucosal injury. In particular, estrogen deficiency exacerbated F-induced enterotoxicity, which provides new explanations for the development and severity of intestinal disease in postmenopausal women with high-F areas.

1. Introduction

The intestinal epithelium, which contains different types of polarized epithelial cells, is the key bridge connecting the body and the external environment (McCarty and Lerner, 2021). Intestinal epithelial cells (IECs) can distinguish between commensal and pathogenic bacteria, which affect immune homeostasis in the intestinal microenvironment (Artis, 2008). As the primary functional unit of IECs, junctional complexes, generally including tight junctions (TJs), adhesion junctions (AJs), and desmosomes, have been paid more attention. Abundant data indicate that dysfunction of junctional complexes is the main determinant of changes in intestinal epithelial permeability (Turner, 2009; Buckley and Turner, 2018). Damage or defects in epithelial permeability hinder the distinguishing ability of epithelial cells and cause displacement of bacteria or toxins (Artis, 2008), which seriously disturbs the balance of intestinal flora, resulting in disruption of homeostasis of the intestinal microenvironment, thereby causing inflammatory disorders, diabetes, and other diseases (Chelakkot et al., 2018).

In addition to naturally high fluoride (F) groundwater, the F contamination crisis, which is also present in industrial wastewater and air, leaves humans and animals confronting an ever-deepening global health risk as the industry develops (Mondal and Chattopadhyay, 2020). Epidemiological investigations have shown that long-term intake of high levels of F can cause damage to human health, impairing the normal physiological functions of skeletal and non-skeletal tissues (Liu et al., 2021). It is worth noting that F pollution caused by the body mainly stems from absorption by the digestive tract, and the small intestine bears its brunt, usually manifesting as motion sickness, vomiting,

* Correspondence to: Henan Key Laboratory of Environmental and Animal Product Safety, Henan University of Science and Technology, Kaiyuan Avenue 263, Luoyang 471000, Henan, People's Republic of China.

E-mail addresses: jinye@stu.haust.edu.cn (Y. Jin), gaoxy@stu.haust.edu.cn (X.-y. Gao), zhaojing19901230@126.com (J. Zhao), tianws0502@126.com (W.-s. Tian), zhangyulings@haust.edu.cn (Y.-l. Zhang), tej1212@haust.edu.cn (E.-j. Tian), zhoubh@haust.edu.cn (B.-h. Zhou), wanghw@haust.edu.cn (H.-w. Wang).

https://doi.org/10.1016/j.ecoenv.2022.114181
Received 2 July 2022; Received in revised form 5 October 2022; Accepted 10 October 2022
Available online 14 October 2022

diarrhea, and abdominal pain (Fu et al., 2022). Based on TJ dysfunction is directly related to the atypical opening of paracellular pathways, which is a key factor in the occurrence of intestinal diseases (Turner, 2009; Landy et al., 2016). And TJs are pivotal to the passage of F through the intestinal mucosa into the body (Buzalaf and Whitford, 2011). Thus, the mechanism of specific intestinal changes after F enters the digestive tract is an attractive problem. Previous studies have shown that oxidative stress, lipid peroxidation, and pyroptosis are some factors responsible for the impairment of gut morphology and structure in response to external F exposure (Chauhan et al., 2011, 2013; Guimaraes de Souza Melo et al., 2021). However, there are little published data on the molecular basis of F-induced structural changes in the intestinal morphology. Here, we provide an in-depth dissection of the junctional mechanisms between epithelial cells, elaborating how F affects gut barrier function through cell-to-cell junctions.

The incidence and severity of various digestive diseases, such as inflammatory bowel disease and intestinal cancer, have been confirmed to have significant gender differences (Nie et al., 2018). Epidemiological surveys have shown that men are more prone to developing intestinal metabolic diseases than women, and postmenopausal women have an increased prevalence of bowel disease compared with age-matched men (Tuo et al., 2011). Obviously, the absence of circulating estrogen increases the risk of intestinal dysfunction (Collins et al., 2017). F has a strong female reproductive toxicity. Excessive F can damage morphology and inhibit cell proliferation by inducing oxidative stress and apoptosis in the ovary, leading to follicular developmental dysplasia (Wang et al., 2017; Bai et al., 2020). Estrogens have been proven to exert a protective effect on the female reproductive system by activating antioxidant enzyme activity and anti-apoptotic pathways (Moor et al., 2004). Combined with our previous experimental studies, microenvironmental destruction is the main mechanism of intestinal epithelial barrier damage and intestinal flora imbalance after F exposure (Liu et al., 2019; Wang et al., 2020). Special attention should be given to the role of the presence of estrogen in the enterotoxicity of F. To date, however, studies on intestinal histopathology and function following high-dose F exposure after estrogen loss have been extremely limited.

To determine the aetiology and potential mechanism of intestinal disease in postmenopausal women with fluorosis areas, this study used ovariectomy (OVX) models to evaluate the effect of estrogen deficiency on the changes in intestinal junctional complex-related proteins in F exposed rats. By further investigating and comparing the specific mechanism of F-induced intestinal mucosal barrier injury, this study provided new views on the potential toxicity of F from the perspective of estrogen.

2. Materials and methods

2.1. Experimental design

A total of 72 healthy female SD rats aged 90-day-old were adaptively fed for a week in the standard animal room with good hygienic and ventilation conditions at 22 °C ± 2 °C under a 12 h light/dark cycle. Similar to our previous study, F exposure models of OVX rats removing the ovaries surgically and non-OVX rats after adding sodium fluoride (NaF) (0, 25, 50, and 100 mg/L, calculated by F ion) in drinking water were treated for 90 days (Yu et al., 2021). That is, all experimental animals were divided into eight groups (n = 9): non-OVX control group, non-OVX F 25 group, non-OVX F 50 group, non-OVX F 100 group, OVX control group, OVX F 25 group, OVX F 50 group, and OVX F 100 group. All animal experiments were approved by the Institutional Animal Experiment Committee of Henan University of Science and Technology, China.

2.2. Histopathological observation

The collected fresh duodenum, jejunum, and ileum were fixed in 4% paraformaldehyde solution for 48 h at room temperature and then taken out, dehydrated by ethanol, and embedded in paraffin. 4 μm serial slices were prepared for hematoxylin-eosin (HE) staining. The stained slides were observed under a light microscope. In each section, six visual fields which randomly selected were used to measure developmental parameters of villus height (VH), crypt depth (CD), and muscle layer thickness.

2.3. Immunohistochemical assay

According to the instructions of the commercialized BrdU staining kit (Servicebio, China), on the 89th day of F treatment, the rats were intraperitoneally injected with 0.2 ml of BrdU solution (10 mg/ml, WGB8010, Servicebio, China) 4 times with an interval of 2 h (Chen et al., 2014; Liu et al., 2019). All experimental rats were sacrificed after the last injection of BrdU for 24 h, and the small intestine tissue were taken for sections preparation. Small intestinal tissue sections were incubated with primary rabbit anti-rat 5-bromo-2-deoxyuridine (BrdU) antibody (1:300 in PBS, GB12051, Servicebio, China) and HRP labeled goat anti-rabbit antibody (1:200 in TBST, GB23301, Servicebio, China). Subsequently, the slices were added with diaminobenzidine (DAB) color solution (G1212, Servicebio, China) after washing three times and were counterstained with hematoxylin (G1004, Servicebio, China). The brown-yellow particles observed indicated that the cells were in the proliferation stage.

2.4. Alcian blue and periodic acid-schiff (AB-PAS) and Periodic acid-schiff (PAS) staining

After the duodenum, jejunum, and ileum tissue sections were dewaxed and rehydrated, they were stained with Alcian blue staining solution (G1049–3, Servicebio, China) for 5 min, periodic acid staining solution (G1049–2, Servicebio, China) for 15 min, Chevron staining solution (G1049–1, Servicebio, China) for 30 min in the dark, and hematoxylin staining solution for 3–5 min (Osho et al., 2017). Eventually, the slices were dehydrated and sealed for observation.

The tissue sections of the duodenum, jejunum, and ileum were directly stained with periodic acid staining solution (G1008–2, Servicebio, China) for 15 min after dewaxing and rehydration (Shi et al., 2017), the following steps were consistent with AB-PAS staining.

2.5. Immunofluorescence analysis

Tissue sections of the duodenum, jejunum, and ileum were dewaxed in xylene and dehydrated with ethanol. After antigen repair in EDTA buffer (pH 8.0), the sections were incubated with 3% BSA for 30 min for removing nonspecific reactions. Afterward, the sections were incubated with primary antibodies claudin-2 (1:500, GB11972, Servicebio, China), occludin (1:500, GB111401, Servicebio, China), zonula occludens-1(ZO-1) (1:500, GB111402, Servicebio, China), E-cadherin (1:500, GB12082, Servicebio, China), and desmoplakin (1:500, GB113491, Servicebio, China) overnight at 4 ℃ and corresponding secondary antibody for 50 min. The nuclei were counterstained with DAPI for 10 min in the dark. Finally, the slides were sealed with an anti-fluorescence quencher and took images under a fluorescence microscope.

2.6. Statistical analysis

Statistical analysis was carried out to perform multi-group comparison and the comparison between non-OVX groups and OVX groups using one-way ANOVA (Tukey post-hoc test) and Student's *t*-test in SPSS 22 software (Inc., Chicago, IL, USA), respectively. All data were expressed as the mean ± SD (standard deviation). $P < 0.05$ and $P < 0.01$ were thought to be statistically significant.

Table 1
Changes in developmental parameters of the duodenum, jejunum, and ileum.

Intestines	Parameters	Non-OVX				OVX			
		Control group	F 25 group	F 50 group	F 100 group	Control group	F 25 group	F 50 group	F 100 group
Duodenum	VH (μm)	482.52 ± 24.68	351.67 ± 35.00 * *	332.42 ± 19.78 * *	280.62 ± 27.86 * *	381.12 ± 15.54$^{\#\#}$	342.55 ± 14.93 *	293.97 ± 26.43 * *$^{\#}$	222.28 ± 14.69 * *$^{\#\#}$
	CD (μm)	175.90 ± 9.54	129.95 ± 14.50 * *	128.80 ± 15.02 * *	115.35 ± 10.94 * *	173.97 ± 20.25	126.58 ± 8.09 * *	118.50 ± 9.40 * *	98.80 ± 11.86 * *$^{\#}$
	VH/CD	2.75 ± 0.22	2.72 ± 0.24	2.62 ± 0.38	2.47 ± 0.41	2.23 ± 0.35$^{\#}$	2.72 ± 0.22	2.51 ± 0.37	2.27 ± 0.22
	Muscle thickness (μm)	100.07 ± 8.21	90.63 ± 4.69	68.87 ± 6.65 * *	59.83 ± 41.41 * *	86.00 ± 5.94$^{\#}$	69.63 ± 3.05 * *$^{\#\#}$	61.08 ± 4.81 * *	36.23 ± 4.44 * *$^{\#\#}$
Jejunum	VH (μm)	371.13 ± 18.39	338.08 ± 23.96 *	306.30 ± 4.53 * *	270.27 ± 13.78 * *	360.22 ± 13.45	335.20 ± 10.83	304.20 ± 9.08 * *	239.55 ± 23.82 * *$^{\#}$
	CD (μm)	135.12 ± 12.70	119.43 ± 9.78	102.98 ± 12.13 * *	96.03 ± 9.02 * *	123.83 ± 6.02	117.97 ± 6.74	101.08 ± 5.98 * *	92.60 ± 3.53 * *$^{\#}$
	VH/CD	2.76 ± 0.21	2.84 ± 0.20	3.02 ± 0.40	2.83 ± 0.23	2.92 ± 0.19	2.85 ± 0.19	3.02 ± 0.16	2.58 ± 0.21 *
	Muscle thickness (μm)	82.38 ± 3.16	64.38 ± 1.71 * *	59.48 ± 4.79 * *	48.17 ± 6.47 * *	66.80 ± 6.41$^{\#\#}$	58.92 ± 2.34$^{\#\#}$	49.68 ± 4.17 * *$^{\#\#}$	38.80 ± 4.71 * *$^{\#}$
Ileum	VH (μm)	322.82 ± 13.97	301.05 ± 8.05 * *	290.02 ± 4.31 * *	266.28 ± 5.43 * *	322.78 ± 8.36	310.43 ± 5.62	288.58 ± 10.42 * *	260.82 ± 19.17 * *
	CD (μm)	133.88 ± 13.51	123.92 ± 6.70	108.78 ± 5.90 * *	98.12 ± 4.79 * *	127.98 ± 7.16	110.68 ± 5.95 * *$^{\#\#}$	103.05 ± 6.78 * *	97.45 ± 8.62 * *
	VH/CD	2.43 ± 0.24	2.44 ± 0.18	2.67 ± 0.13	2.72 ± 0.10	2.53 ± 0.12	2.81 ± 0.15 *$^{\#\#}$	2.81 ± 0.11 *	2.69 ± 0.22
	Muscle thickness (μm)	72.70 ± 2.64	63.30 ± 2.06 * *	58.42 ± 4.27 * *	42.32 ± 1.35 * *	64.15 ± 2.42$^{\#\#}$	47.77 ± 4.15 * *$^{\#\#}$	39.75 ± 3.43 * *$^{\#\#}$	36.72 ± 4.51 * *$^{\#}$

VH: villus height. CD: crypt depth. VH/CD: the ratio of villi area to crypt depth. All data were expressed as mean ± SD (n = 6). "* " indicates statistically significant difference between the control group and the F exposure group by using one-way ANOVA, followed by Tukey post-hoc test (*P < 0.05 and **P < 0.01); "#" indicates statistically significant difference between the non-OVX group and the OVX group under the same F treatment by using Student's t-test (#P < 0.05 and ##P < 0.01).

3. Results

3.1. Effect of F on the development parameters in the duodenum, jejunum, and ileum

In Table 1, F exposure significantly reduced duodenal VH and CD ($P < 0.01$) by 27.12% and 26.12% in the non-OVX F 25 group, 31.11% and 26.78% in the non-OVX F 50 group and 41.84% and 34.42% in the non-OVX F 100 group, respectively. Duodenal VH and CD were also reduced in OVX all F treated groups ($P < 0.05$ or $P < 0.01$), by 10.12% and 27.24%, 22.87% and 31.88%, and 41.68% and 43.21%, respectively. Likewise, the duodenal muscle thickness was decreased by 31.18% and 40.21% in the non-OVX F 50 and 100 groups ($P < 0.01$); while that of OVX F all treatment groups was decreased by 19.03%, 28.97%, and 57.87%, respectively ($P < 0.01$). Additionally, in the presence of estrogen deficiency, duodenal VH was further reduced by 21.01% in the control group ($P < 0.01$), 11.57% in the F 50 group ($P < 0.05$), and 20.79% ($P < 0.01$) in the F 100 group. CD from duodenum in the OVX groups was significantly decreased by 14.35% than that of non-OVX groups with the addition of 100 mg/L F ($P < 0.05$). Estrogen deficiency further reduced duodenal villus height/crypt depth (VH/CD) by 18.99% in the control group and significantly decreased muscle thickness by 14.06% in the control, 23.17% in the F 25%, and 39.44% in the F 100 groups ($P < 0.05$ or $P < 0.01$), respectively.

In the jejunum, F exposure significantly reduced VH and muscle thickness by 8.91% and 21.85% in the non-OVX F 25 group ($P < 0.05$ or $P < 0.01$), 17.47% and 27.8% in the non-OVX F 50 group ($P < 0.01$), and 27.18% and 41.53% in the non-OVX F 100 group ($P < 0.01$), respectively; the VH and muscle thickness of OVX groups were also markedly decreased ($P < 0.01$), especially by 15.55% and 25.62% in the OVX F 50 group and 33.5% and 41.92% in the OVX F 100 group. When adding 50 and 100 mg/L F, CD was significantly decreased by 23.78% and 28.93% in the non-OVX groups ($P < 0.01$) and by 18.37% and 25.22% in OVX groups ($P < 0.01$), respectively. VH/CD was significantly reduced by 11.41% in the OVX F 100 group compared to the OVX control group ($P < 0.05$). Furthermore, adding 100 mg/L of F, the lack of estrogen further reduced VH by 11.37% and CD by 3.58% in jejunum ($P < 0.05$). Muscle thickness was further reduced by 18.92% in the control group, 8.49% in the F 25, 16.48% in the F 50%, and 19.45% in the F 100 group with the presence of estrogen deficiency ($P < 0.05$ or $P < 0.01$).

In the ileum, excessive F significantly decreased VH and muscle thickness by 6.74% and 12.93%, 10.16% and 19.65%, and 17.51% and 41.79% in non-OVX all F treatment groups, respectively; CD by 18.75% in the non-OVX F 50 group and 26.71% in the non-OVX F 100 group ($P < 0.01$). F also reduced VH by 10.6% in the OVX F 50 group and 19.2% in the OVX F 100 group; CD and muscle thickness by 13.52% and 25.54% in the OVX F 25, 19.48% and 38.04% in the OVX F 50%, and 23.86% and 42.76% in the OVX F100 group ($P < 0.01$). Excessive F changed VH/CD in the OVX F 25 and 50 groups ($P < 0.05$). Likewise, estrogen deficiency further changed VH/CD and decreased CD by 10.68% when adding 25 mg/L of F ($P < 0.01$). Meanwhile, muscle thickness was also further reduced by 11.76% in the control group, 24.54% in the F 25, 31.95% in the F 50%, and 13.23% in the F 100 group when estrogen was absent ($P < 0.05$ or $P < 0.01$).

3.2. Morphological structure of the duodenum, jejunum, and ileum in response to F exposure

As shown in Fig. S1, the intestinal mucosa of the duodenum, jejunum, and ileum in the non-OVX control group atrophied with increasing doses of F, specifically as villi became shorter and thinner, and crypts became shallower. Muscle thickness decreased significantly after adding the dose of 100 mg/L of F. F exposure induced histopathological lesions of the small intestine tissues were aggravated in the OVX groups compared with those in the non-OVX groups.

3.3. Proliferation of intestinal epithelial cells in the duodenum, jejunum, and ileum after F exposure

The analysis of BrdU in the duodenum, jejunum, and ileum tissues was shown in Fig. 1. In the non-OVX control groups, BrdU-labelled the duodenum, jejunum, and ileum tissues presented positive expression in the nucleus (Fig. S2). F exposure markedly decreased the percentage of positive expression in the small intestine ($P < 0.01$), by 23.18%, 34.46% and 41.32% in the duodenal non-OVX F 25 group, F 50 group and F 100 group, 23.86%, 35.47% and 54.69% in the jejunal non-OVX all F

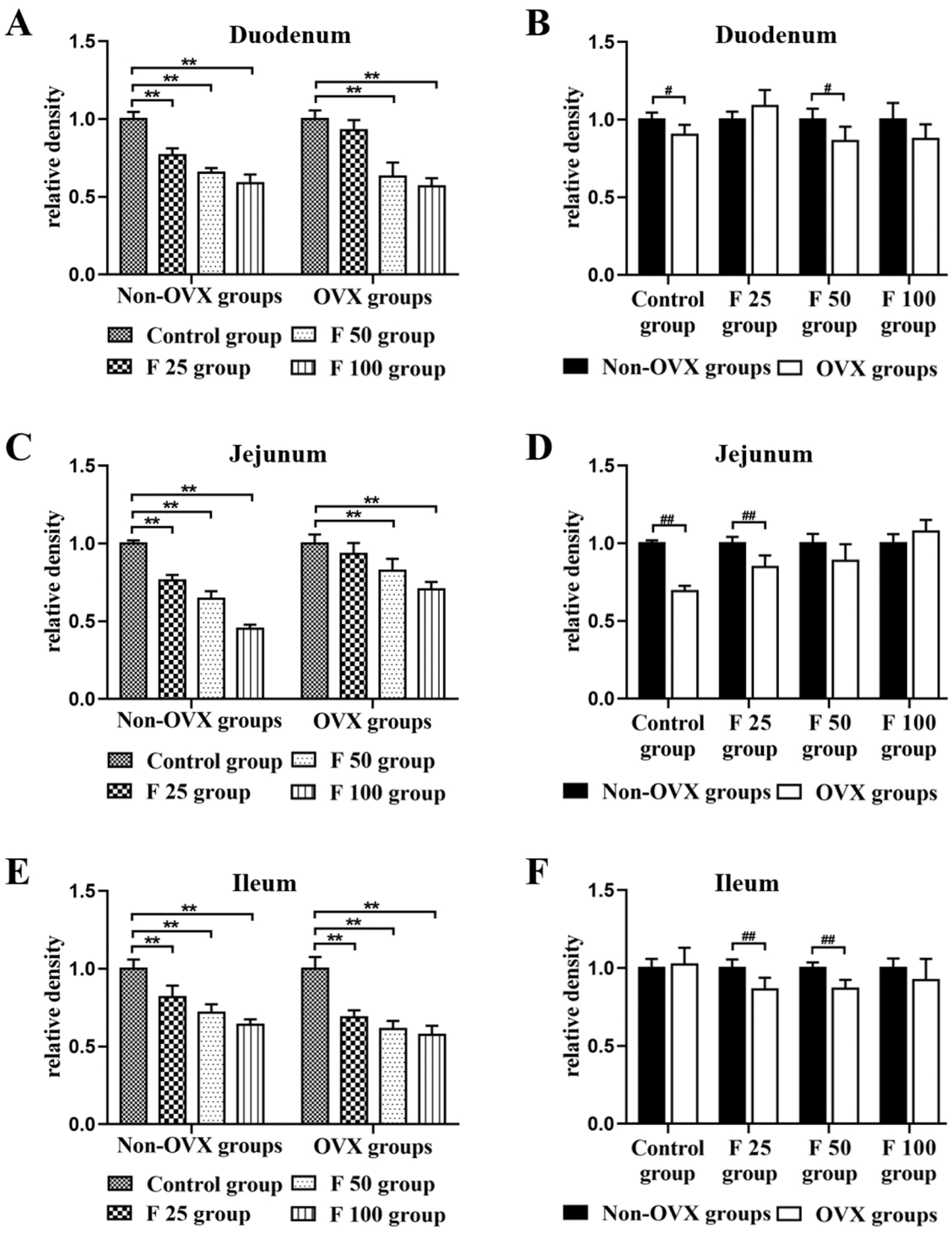

Fig. 1. Analysis of small intestinal cells proliferation ability in female rats by BrdU labeling. (A), (C), and (E) are relative densities of BrdU labelled positive expression in the duodenum, jejunum, and ileum of non-OVX and OVX rats. (B), (D), and (F) are the comparison between non-OVX and OVX groups of BrdU labelled positive expression in the duodenum, jejunum, and ileum. All data were expressed as mean ± SD (n = 6). "* " indicates statistically significant difference between the control group and the F exposure group by using one-way ANOVA, followed by Tukey post-hoc test (* $P < 0.05$ and ** $P < 0.01$); "$^{\#}$" indicates statistically significant difference between the non-OVX group and the OVX group under the same F treatment by using Student's *t*-test ($^{\#}P < 0.05$ and $^{\#\#}P < 0.01$).

treatment groups, and 18.32%, 28.18%, and 36.1% in the ileal non-OVX all F treatment groups, respectively; by 36.99% and 43.21% in the duodenum OVX F 50 and F 100 groups, 17.58% and 29.26% in the jejunum OVX F 50 and 100 groups, and 31.21%, 38.84% and 42.54% in the ileal OVX F treatment group, respectively (Fig. S2, Fig. 1A, C, and E). In addition, the proportion of positive expression of BrdU in the OVX groups was decreased more than that in the non-OVX groups, especially by 9.85% and 13.8% in the duodenum control and F 50 groups, 30.82% and 15.27% in the jejunum control and F 25 groups, and 13.66% and 13.14% in the ileum F 25 and 50 groups ($P < 0.05$ or $P < 0.01$) (Fig. S2, Fig. 1B, D, and F), suggesting that estrogen deficiency further inhibited the proliferation of intestinal epithelial cells.

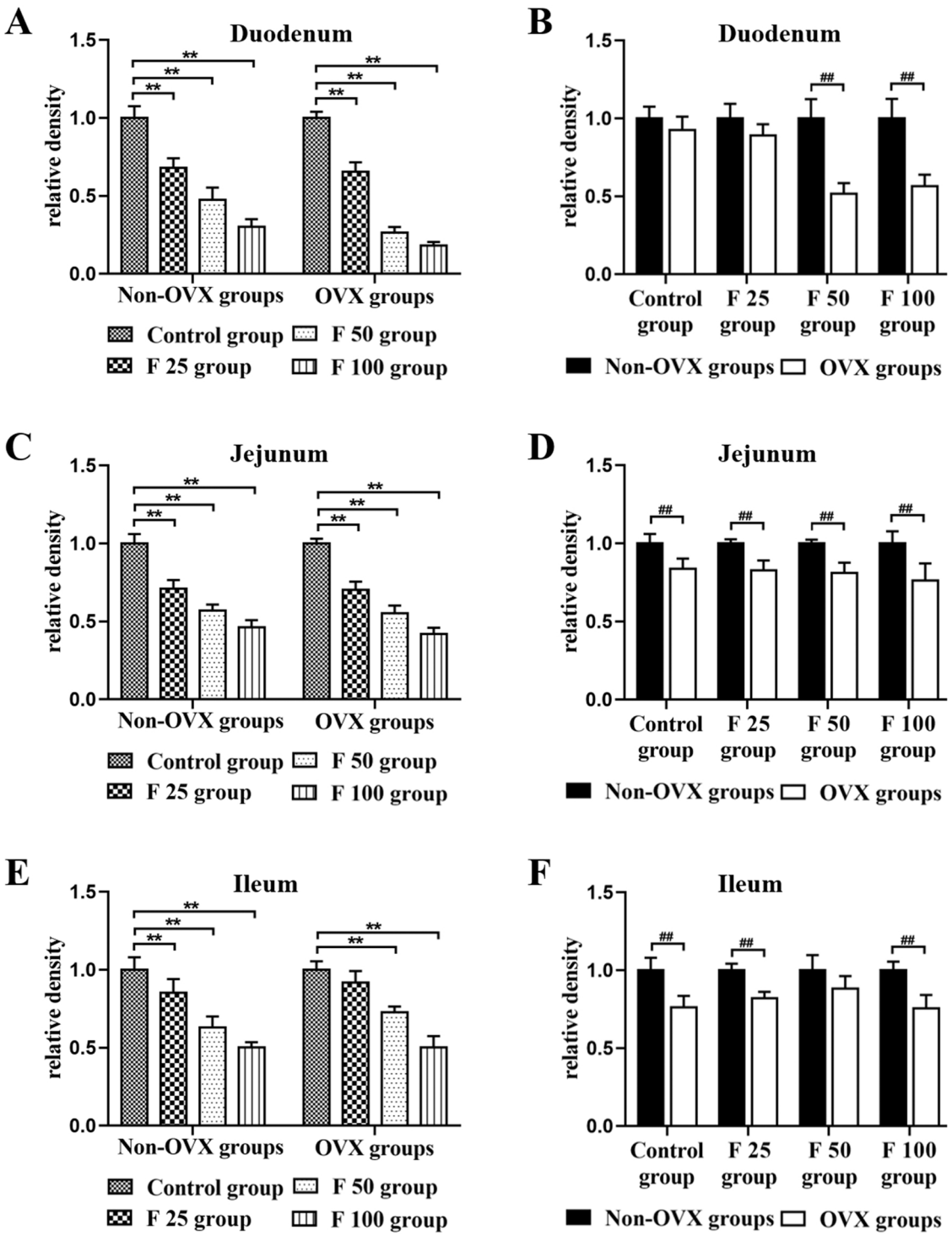

Fig. 2. Effect of F on the goblet cells number of the small intestine in female rats by AB-PAS staining. (A), (C), and (E) are relative densities of goblet cells in the duodenum, jejunum, and ileum of non-OVX and OVX rats. (B), (D), and (F) are the comparison between non-OVX and OVX groups of goblet cells in the duodenum, jejunum, and ileum. All data were expressed as mean ± SD (n = 6). "* " indicates statistically significant difference between the control group and the F exposure group by using one-way ANOVA, followed by Tukey post-hoc test (* $P < 0.05$ and ** $P < 0.01$); "$^{\#}$" indicates statistically significant difference between the non-OVX group and the OVX group under the same F treatment by using Student's *t*-test ($^{\#}P < 0.05$ and $^{\#\#}P < 0{\cdot}01$).

3.4. Number of goblet cells in the duodenum, jejunum, and ileum after F exposure

The number of goblet cells in the duodenum, jejunum, and ileum was detected by AB-PAS staining after F exposure (Fig. S3). As illustrated in Fig. 2, excessive F significantly reduced the number of goblet cells ($P < 0.01$) by 32.03%, 52.56%, and 69.93% in the duodenal non-OVX F 25, F 50, and F 100 group and by 34.55%, 73.72%, and 81.82% in the OVX F treatment group, respectively; and by 28.9%, 43.08%, and 53.64% in the jejunal non-OVX F treatment groups and 29.76%, 44.84%, and 58.11% in the OVX F treatment groups, respectively (Fig. S3, Fig. 2A and C). Likewise, F exposure markedly reduced ($P < 0.01$) the number of goblet cells in the ileum, particularly by 14.84%, 36.93%, and 49.67% in the non-OVX F-treated groups and by

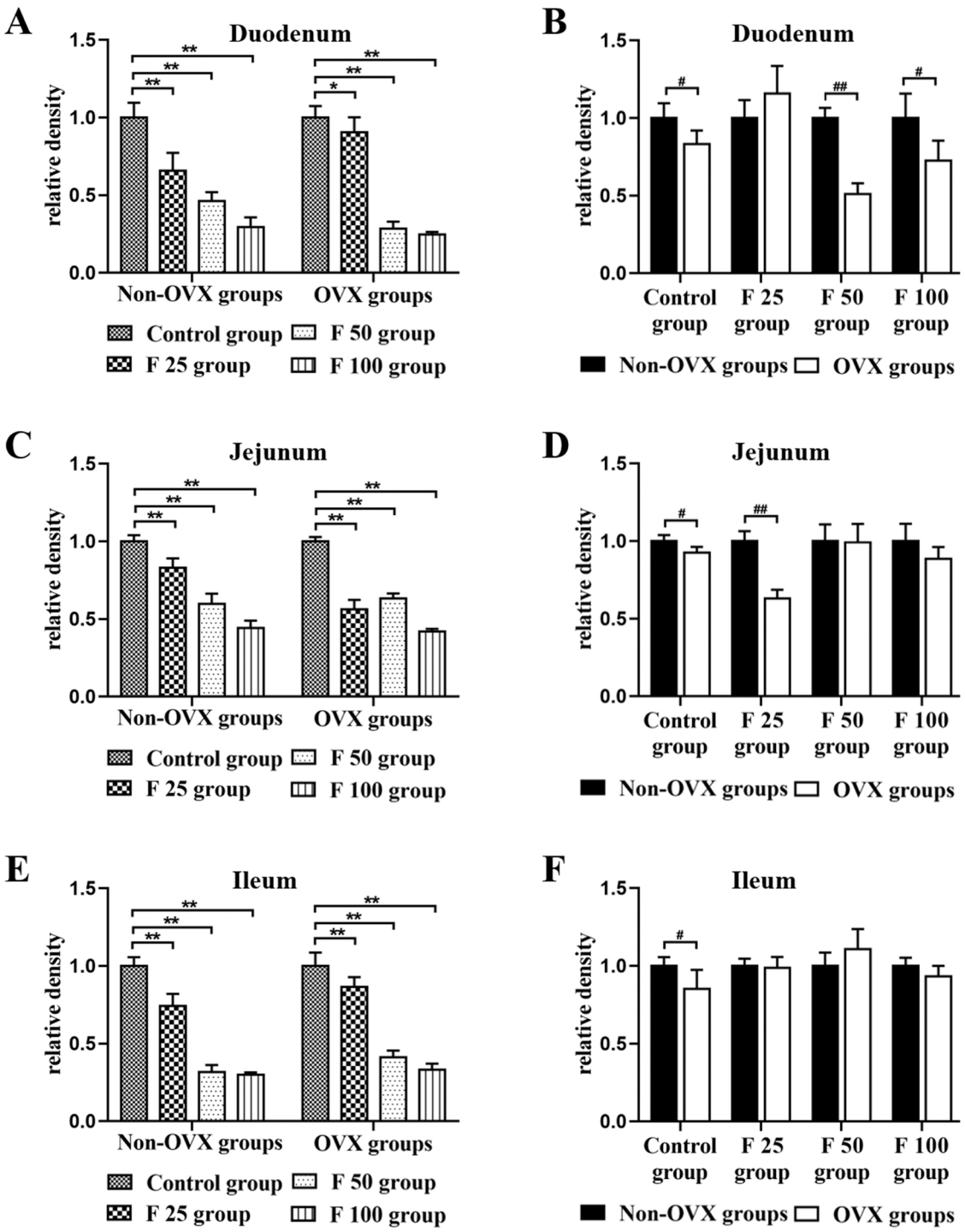

Fig. 3. Effect of F on the glycoprotein expression of the small intestine in female rats by PAS staining. (A), (C), and (E) are relative densities of glycoproteins in the duodenum, jejunum, and ileum of non-OVX and OVX rats. (B), (D), and (F) are the comparison between non-OVX and OVX groups of glycoproteins in the duodenum, jejunum, and ileum. All data were expressed as mean ± SD (n = 6). "* " indicates statistically significant difference between the control group and the F exposure group by using one-way ANOVA, followed by Tukey post-hoc test (* $P < 0.05$ and ** $P < 0.01$); "$^{\#}$" indicates statistically significant difference between the non-OVX group and the OVX group under the same F treatment by using Student's *t*-test ($^{\#}P < 0.05$ and $^{\#\#}P < 0.01$).

27.36% and 49.74% in the OVX F 50 and 100 groups (Fig. S3 and Fig. 2E). In addition, estrogen deficiency further reduced ($P < 0.01$) the number of goblet cells by 48.26% and 43.53% in the duodenum F 50 and F 100 groups, respectively; in the jejunum control group and all F treated groups, the reduction was 16.21%, 17.23%, 18.92% and 23.77% ($P < 0.01$); while in the ileum control group, F 25 and F 100 group, the reduction was 23.77%, 18.02% and 24.47% ($P < 0.01$), respectively (Fig. S3, Fig. 2B, D, and F). These results showed F exposure reduced the number of goblet cells in the small intestine in a dose-dependent manner, and the reduction was more pronounced under the state of estrogen deficiency.

3.5. *Distribution of glycoproteins in the duodenum, jejunum, and ileum after F exposure*

PAS staining was employed to identify the distribution of

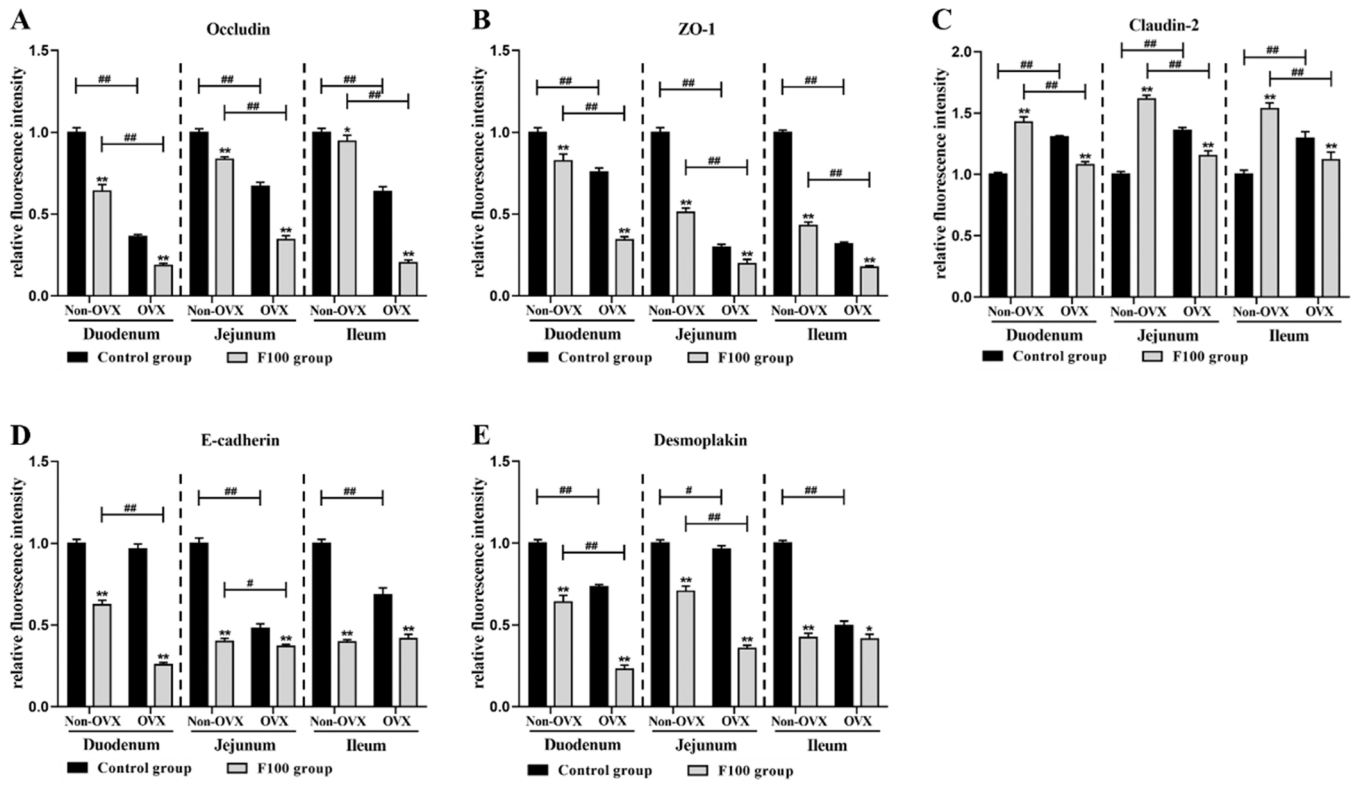

Fig. 4. Immunofluorescence analysis the expression of occludin, ZO-1, claudin-2, E-cadherin, and desmoplakin of the small intestine in female rats. The relative fluorescence intensity of occludin (A), ZO-1 (B), claudin-2 (C), E-cadherin (D), and desmoplakin (E) of the small intestine in the non-OVX and OVX rats, respectively. All data were expressed as mean ± SD (n = 6). "* " indicates statistically significant difference between the control group and the F 100 group by using Student's *t*-test (* $P < 0.05$ and ** $P < 0.01$); "$^{\#}$" indicates statistically significant difference between the non-OVX group and the OVX group under the same F treatment by using Student's *t*-test ($^{\#}P < 0.05$ and $^{\#\#}P < 0{\cdot}01$).

glycoproteins in the duodenum, jejunum, and ileum after F exposure (Fig. S4). As depicted in Fig. 3, the relative density of glycoproteins from duodenum was decreased ($P < 0.05$ or $P < 0.01$) significantly with increasing F dose by 34.13%, 53.68%, and 70.73% in the non-OVX F 25, 50, and 100 groups; 9.48%, 71.53%, and 75.31% in OVX all F treatment groups (Fig. S4, Fig. 3A, C, and E). Similarly, the relative density of glycoproteins in the jejunum was also reduced by 16.98%, 40.19%, and 55.76% in the non-OVX F treated groups ($P < 0.01$); 43.63%, 36.67%, and 58.02% in the OVX F treated groups ($P < 0.01$); by 25.68%, 68.28%, and 70.16% in the ileal non-OVX F treated groups ($P < 0.01$) and 13.4%, 58.7%, and 66.92% in the ileal OVX F treated groups ($P < 0.01$) (Fig. S4, Fig. 3A, C, and E). In addition, in the state of estrogen deficiency, the relative density of glycoproteins from duodenum was further decreased ($P < 0.05$ or $P < 0.01$), particularly by 16.85% in the control, 48.93% in the F 50%, and 27.52% in the F 100 groups (Fig. S4 and Fig. 3B). The expression of glycoproteins in the jejunal OVX control and F 25 groups was decreased by 7.44% and 37.11% ($P < 0.05$ or $P < 0.01$) compared with those in the jejunal non-OVX control and F 25 groups (Fig. S4 and Fig. 3D). After OVX, glycoproteins expression was significantly reduced ($P < 0.05$) by 14.81% in the ileal control group (Fig. S4 and Fig. 3F). Obviously, the lack of estrogen further inhibited glycoproteins secretion in the small intestine.

3.6. Immunofluorescence analysis the protein expression levels of TJs, AJs, and desmosomes in the duodenum, jejunum, and ileum

The protein expression levels of occludin, ZO-1, and claudin-2 in the duodenum, jejunum, and ileum were analyzed by immunofluorescence (Figs. S5 and S6). As shown in Fig. 4, in the absence of OVX, the protein expression levels of occludin and ZO-1 were down-regulated by 36.01% and 17.43% in duodenum, 16.49% and 48.95% in jejunum, 5.4% and 56.97% in ileum ($P < 0.05$ or $P < 0.01$), and the expression level of claudin-2 was up-regulated by 42.69%, 61.59%, and 53.63% in the small intestine ($P < 0.01$), respectively, when F 100 mg/L was added (Fig. 4A, B, and C). F supplementation after OVX resulted in down-regulation of occludin, ZO-1, and claudin-2 protein expression levels by 48.39%, 55.06%, and 17.42% in the duodenum ($P < 0.01$); 48.52%, 33.98%, and 15.24% in the jejunum ($P < 0.01$); and 68.4%, 44.64%, and 13.4% in the ileum ($P < 0.01$), respectively (Fig. 4A, B, and C). In the absence of estrogen, the protein expression levels of occludin and ZO-1 decreased by 63.92% and 24.21%, 33.19% and 70.39%, and 36.36% and 68.41% in the duodenum, jejunum, and ileum control groups ($P < 0.01$); by 70.89% and 58.73%, 58.84% and 61.77%, and 78.77% and 59.24% in the duodenum, jejunum, and ileum F 100 groups ($P < 0.01$) (Fig. 4A and B). Compared with the non-OVX control group, the protein expression level of claudin-2 was increased ($P < 0.01$) by 30.56%, 35.96%, and 29.34% in the OVX control group of small intestinal tissues, respectively. Meanwhile, the protein expression level of claudin-2 in the OVX F 100 group of small intestinal tissues was decreased ($P < 0.01$) by 24.42%, 28.68%, and 27.07% compared with that in the non-OVX F 100 group (Fig. 4C).

The protein expression levels of E-cadherin and desmoplakin in the duodenum, jejunum, and ileum were assessed (Fig. 4D and E). After the 100 mg/L of F was added, the protein expression levels of E-cadherin and desmoplakin were significantly down-regulated by 37.69% and 36.02%, 60.09% and 29.38%, and 60.43% and 57.75% in the duodenum, jejunum, and ileum of non-OVX rats ($P < 0.01$), respectively; meanwhile, they were down-regulated by 73.3% and 68.73%, 23.03% and 62.9%, and 39.03% and 16.23% in the small intestine of OVX rats ($P < 0.05$ or $P < 0.01$), respectively. Under the condition of estrogen deficiency, the expression level of E-cadherin protein in the jejunal and ileal control group was significantly decreased ($P < 0.05$ or $P < 0.01$) by

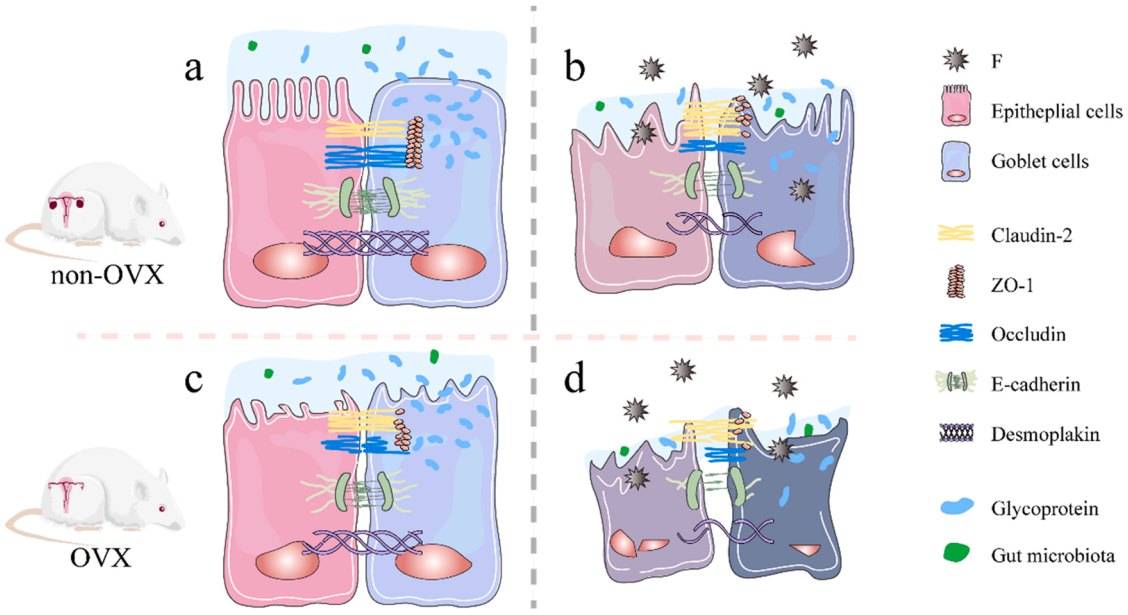

Fig. 5. Schematic diagram of estrogen aggravating F-induced intestinal mucosal barrier damage. Intestinal mucosal barrier structure was intact in non-OVX rats (a). Excessive F intake severely impaired intestinal mucosal barrier (b). Estrogen deficiency affected the structure and function of intestinal mucosal barrier of OVX rats to some extent than those in non-OVX rats (c). F-induced changes in the intestinal mucosal barrier of OVX rats were further exacerbated under estrogen deficiency (d).

52.07% and 31.54% ($P < 0.01$), while the expression level of desmoplakin protein in the small intestinal control group was markedly downregulated ($P < 0.05$ or $P < 0.01$) by 26.65%, 3.81%, and 50.36%. Meanwhile, the protein expression levels of E-cadherin and desmoplakin after OVX were distinctly decreased ($P < 0.01$) by 58.58% and 64.27% in duodenum, 7.58% and 49.39% in jejunum.

4. Discussion

Due to dietary and geographical differences, people have different levels of F intake. Based on the gut as the main organ that absorbs F, this study investigated the role of estrogen deficiency in F-induced intestinal tissue damage by adding F to drinking water. The intestinal epithelium, as a physical barrier, is essential for maintaining intestinal homeostasis (Maloy and Powrie, 2011). The VH and CD of the intestinal epithelium and muscular thickness are consistently evaluated as important indicators of intestinal digestive and absorptive capacity (Zhao et al., 2021). This study showed that excessive F could seriously damage small intestinal tissues and change intestinal development parameters, which may weaken the absorption of nutrients in the body. In good health, intestinal epithelial cells are constantly supplemented and renewed by stem cells in the crypt, and move upward along the crypt-villus axis to fill the villi, thus maintaining normal intestinal function (Luo et al., 2013). F inhibited the proliferation of intestinal epithelial cells and made the cells in villi unable to renew continuously, which may account for the reduced intestinal development parameters induced by F. Damage to intestinal tissues and intestinal epithelial cells may be associated with an F-induced reduction in antioxidant capacity, leading to ROS generate and cytochrome C release, further accelerating cell damage and apoptosis (Sana et al., 2017; Zhou et al., 2020).

The mucus and epithelial cells of the gastrointestinal tract are the main gatekeepers and controllers (Pelaseyed et al., 2014). Fresh mucus, mainly composed of mucin glycoproteins, is continuously secreted from goblet cells to serve as a mediator that protects, lubricates, and transports contents of the lumen and epithelial lining (Bhatia et al., 2015; Diebel et al., 2015). The integrity of mucus and epithelium is essential for resisting intestinal diseases (Luo et al., 2013; Zhu et al., 2022). Our previous studies indicated that excessive F damages the intestinal immune function in the colon, cecum, and rectum tissues (Liu et al., 2019; Wang et al., 2020; Zhu et al., 2022). In this study, we found that both the number of goblet cells and the ability of glycoprotein secretion were significantly reduced. After OVX, damage to the intestinal mucosal barrier was more pronounced. It was clear that estrogen deficiency exacerbates F enterotoxicity. Estrogen alleviates cell death by activating anti-apoptotic pathways, effectively against oxidative damage (Moor et al., 2004). Estrogen deficiency aggravates the loss of F-induced antioxidant defense system, further increasing the risk of intestinal malabsorption and exhaustion.

TJs, which bind completely to the cytoskeleton of adjacent intestinal cells, are apical components of intercellular junctional complexes in epithelial cells (Sharma et al., 2018). From a microscopic viewpoint, TJ proteins participate in the protection of intestinal epithelial cells from microbial colonization and are involved in developmental, physiological, and pathological processes (Lerner and Matthias, 2015). And the realisation of its function is inseparable from the integration of TJ proteins, such as occludin, ZO-1, and claudin-2 (McCarty and Lerner, 2021). Previous studies have shown that abnormal expression of ZO-1, occludin, and claudin-2 mostly occurs when intestinal homeostasis is disrupted and immune function is impaired (Rosenthal et al., 2010; Slifer and Blikslager, 2020). Our study found that high F also led to the disturbance of TJ proteins expression and increased permeability between intestinal epithelial cells, manifested as widening intercellular spaces, which is the cause of mucosal barrier dysfunction. The integrity of the TJs was further destroyed after OVX, which may be related to estrogen-dependent energy metabolism through the nuclear ER (Choi et al., 2018; Tran et al., 2021). Among them, calcium malabsorption was thought to be the key factor for the imbalance in claudin-2 protein expression induced by co-treatment with F and OVX (Christakos et al., 2011).

TJs assembly require the assistance of AJs. E-cadherin, as a representative of AJ proteins in the epithelium, is usually significantly involved in tumor invasiveness, metastatic dissemination, and poor patient outcomes (Onder et al., 2008). In this study, a trend towards a marked reduction in the distribution of E-cadherin in the gut was observed after co-treatment with OVX and F, implying that estrogen deficiency may increase the gap between epithelial cells. Additionally, we found that the decline in desmoplakin may be related to the change in E-cadherin, which is the result of the downregulation of E-cadherin

(Shafraz et al., 2018). Imbalance in the expression of a series of proteins in junctional complexes inevitably affects the mucosal barrier integrity. Dysregulation of this barrier can lead to widespread adverse consequences, such as inflammatory bowel disease, celiac disease, obesity, and type I diabetes (Collins et al., 2017; Chelakkot et al., 2018). Our study suggested that the combination of F and estrogen deficiency aggravated intestinal mucosal damage and toxicity, which provides new explanations for the development and severity of intestinal disease in postmenopausal women with high-F areas (Nie et al., 2018).

5. Conclusion

In conclusion, as shown in Fig. 5, excessive F disrupted cell-to-cell junctions by disturbing the expression of TJ, AJ, and desmosomal proteins, induced intestinal epithelial cell injury and mucosal morphological changes in the small intestine, resulting in the reduction of glycoproteins secretion. These changes were further aggravated after OVX. These results would provide a new explanation for the development and severity of intestinal disease in postmenopausal women with high-F areas.

CRediT authorship contribution statement

Ye Jin: Writing – original draft, Formal analysis, Data curation, Visualization. **Xiao-ying Gao:** Investigation, Methodology, Validation. **Jing Zhao:** Funding acquisition, Software. **Wei-shun Tian:** Investigation, Supervision. **Yu-ling Zhang:** Validation, Supervision. **Er-jie Tian:** Funding acquisition, Supervision. **Bian-hua Zhou:** Investigation, Validation. **Hong-wei Wang:** Conceptualization, Project administration.

Declaration of Competing Interest

The authors declare that they have no known competing financial interests or personal relationships that could have appeared to influence the work reported in this paper.

Data Availability

Data will be made available on request.

Acknowledgments

This work was financially supported by the National Natural Science Foundation of China (Grant No. 32102740), Henan Province's Key Research and Development and Promotion Project (Grant No. 212102110361), and Henan University of Science and Technology Doctoral Research Startup Fund Project (Grant No. 13480090).

Appendix A. Supporting information

Supplementary data associated with this article can be found in the online version at doi:10.1016/j.ecoenv.2022.114181.

References

Artis, D., 2008. Epithelial-cell recognition of commensal bacteria and maintenance of immune homeostasis in the gut. Nat. Rev. Immunol. 8, 411–420. https://doi.org/10.1038/nri2316.

Bai, R., et al., 2020. Associations of fluoride exposure with sex steroid hormones among U.S. children and adolescents, NHANES 2013-2016. Environ. Pollut. 260, 114003 https://doi.org/10.1016/j.envpol.2020.114003.

Bhatia, S., et al., 2015. Galacto-oligosaccharides may directly enhance intestinal barrier function through the modulation of goblet cells. Mol. Nutr. Food Res 59, 566–573. https://doi.org/10.1002/mnfr.201400639.

Buckley, A., Turner, J.R., 2018. Cell biology of tight junction barrier regulation and mucosal disease. Cold Spring Harb. Perspect. Biol. 10 https://doi.org/10.1101/cshperspect.a029314.

Buzalaf, M.A.R., Whitford, G.M., 2011. Fluoride metabolism. Monogr. Oral. Sci. 22, 20–36. https://doi.org/10.1159/000325107.

Chauhan, S.S., et al., 2011. Modulation of lipid peroxidation and antioxidant defense systems in rat intestine by subchronic fluoride and ethanol administration. Alcohol 45, 663–672. https://doi.org/10.1016/j.alcohol.2010.10.008.

Chauhan, S.S., et al., 2013. Ethanol and age enhances fluoride toxicity through oxidative stress and mitochondrial dysfunctions in rat intestine. Mol. Cell Biochem 384, 251–262. https://doi.org/10.1007/s11010-013-1804-6.

Chelakkot, C., et al., 2018. Mechanisms regulating intestinal barrier integrity and its pathological implications. Exp. Mol. Med 50, 1–9. https://doi.org/10.1038/s12276-018-0126-x.

Chen, L., et al., 2014. Distribution of BrdU label-retaining cells in eccrine sweat glands and comparison of the percentage of BrdU-positive cells in eccrine sweat glands and in epidermis in rats. Arch. Dermatol. Res 306 (2), 157–162. https://doi.org/10.1007/s00403-013-1397-7.

Choi, Y.S., et al., 2018. Estrogen reinforces barrier formation and protects against tumor necrosis factor alpha-induced barrier dysfunction in oral epithelial cells. J. Periodontal Implant Sci. 48, 284–294. https://doi.org/10.5051/jpis.2018.48.5.284.

Christakos, S., et al., 2011. Vitamin D and intestinal calcium absorption. Mol. Cell Endocrinol. 347, 25–29. https://doi.org/10.1016/j.mce.2011.05.038.

Collins, F.L., et al., 2017. Temporal and regional intestinal changes in permeability, tight junction, and cytokine gene expression following ovariectomy-induced estrogen deficiency. Physiol. Rep. 5 https://doi.org/10.14814/phy2.13263.

Diebel, M.E., et al., 2015. Estrogen modulates intestinal mucus physiochemical properties and protects against oxidant injury. J. Trauma Acute Care Surg. 78, 94–99. https://doi.org/10.1097/TA.0000000000000499.

Fu, R., et al., 2022. Exercise alleviated intestinal damage and microbial disturbances in mice exposed to fluoride. Chemosphere 288, 132658. https://doi.org/10.1016/j.chemosphere.2021.132658.

Guimaraes de Souza Melo, C., et al., 2021. Global proteomic profile integrated to quantitative and morphometric assessment of enteric neurons: investigation of the mechanisms involved in the toxicity induced by acute fluoride exposure in the duodenum. Neurotox. Res 39, 800–814. https://doi.org/10.1007/s12640-020-00296-9.

Landy, J., et al., 2016. Tight junctions in inflammatory bowel diseases and inflammatory bowel disease associated colorectal cancer. World J. Gastroenterol. 22, 3117–3126. https://doi.org/10.3748/wjg.v22.i11.3117.

Lerner, A., Matthias, T., 2015. Changes in intestinal tight junction permeability associated with industrial food additives explain the rising incidence of autoimmune disease. Autoimmun. Rev. 14, 479–489. https://doi.org/10.1016/j.autrev.2015.01.009.

Liu, J., et al., 2019. Intestinal barrier damage involved in intestinal microflora changes in fluoride-induced mice. Chemosphere 234, 409–418. https://doi.org/10.1016/j.chemosphere.2019.06.080.

Liu, P., et al., 2021. Co-exposure to fluoride and arsenic disrupts intestinal flora balance and induces testicular autophagy in offspring rats. Ecotoxicol. Environ. Saf. 222, 112506 https://doi.org/10.1016/j.ecoenv.2021.112506.

Luo, Q., et al., 2013. Suppressive effects of dietary high fluorine on the intestinal development in broilers. Biol. Trace Elem. Res 156, 153–165. https://doi.org/10.1007/s12011-013-9845-y.

Maloy, K.J., Powrie, F., 2011. Intestinal homeostasis and its breakdown in inflammatory bowel disease. Nature 474, 298–306. https://doi.org/10.1038/nature10208.

McCarty, M.F., Lerner, A., 2021. Perspective: prospects for nutraceutical support of intestinal barrier function. Adv. Nutr. 12, 316–324. https://doi.org/10.1093/advances/nmaa139.

Mondal, P., Chattopadhyay, A., 2020. Environmental exposure of arsenic and fluoride and their combined toxicity: A recent update. J. Appl. Toxicol. 40, 552–566. https://doi.org/10.1002/jat.3931.

Moor, A.N., et al., 2004. A putative mitochondrial mechanism for antioxidative cytoprotection by 17beta-estradiol. Exp. Eye Res 78 (5), 933–944. https://doi.org/10.1016/j.exer.2004.01.001.

Nie, X., et al., 2018. Effects of estrogen on the gastrointestinal tract. Dig. Dis. Sci. 63, 583–596. https://doi.org/10.1007/s10620-018-4939-1.

Onder, T.T., et al., 2008. Loss of E-cadherin promotes metastasis via multiple downstream transcriptional pathways. Cancer Res 68, 3645–3654. https://doi.org/10.1158/0008-5472.CAN-07-2938.

Osho, S.O., et al., 2017. Comparison of goblet cell staining methods in jejunal mucosa of Turkey poults. Poult. Sci. 96 (3), 556–559. https://doi.org/10.3382/ps/pew324.

Pelaseyed, T., et al., 2014. The mucus and mucins of the goblet cells and enterocytes provide the first defense line of the gastrointestinal tract and interact with the immune system. Immunol. Rev. 260, 8–20. https://doi.org/10.1111/imr.12182.

Rosenthal, R., et al., 2010. Claudin-2, a component of the tight junction, forms a paracellular water channel. J. Cell Sci. 123, 1913–1921. https://doi.org/10.1242/jcs.060665.

Sana, S., et al., 2017. Vesicular melatonin efficiently downregulates sodium fluoride-induced rat hepato- and broncho-TNF-α, TGF-β expressions, and associated oxidative injury: a comparative study of liposomal and nanoencapsulated forms. Int J. Nanomed. 12, 4059–4071. https://doi.org/10.2147/IJN.S124119.

Shafraz, O., et al., 2018. E-cadherin binds to desmoglein to facilitate desmosome assembly. Elife 7. https://doi.org/10.7554/eLife.37629.

Sharma, D., et al., 2018. Pyrin inflammasome regulates tight junction integrity to restrict colitis and tumorigenesis. e8 Gastroenterology 154, 948–964. https://doi.org/10.1053/j.gastro.2017.11.276.

Shi, J., et al., 2017. Intestinal microbiota contributes to colonic epithelial changes in simulated microgravity mouse model. FASEB J. 31 (8), 3695–3709. https://doi.org/10.1096/fj.201700034R.

Slifer, Z.M., Blikslager, A.T., 2020. The integral role of tight junction proteins in the repair of injured intestinal epithelium. Int J. Mol. Sci. 21 https://doi.org/10.3390/ijms21030972.

Tran, A., et al., 2021. Estrogen-related receptor alpha (ERRα) is a key regulator of intestinal homeostasis and protects against colitis. Sci. Rep. 11 (1), 15073. https://doi.org/10.1038/s41598-021-94499-5.

Tuo, B., et al., 2011. Estrogen regulation of duodenal bicarbonate secretion and sex-specific protection of human duodenum. Gastroenterology 141 (3), 854–863. https://doi.org/10.1053/j.gastro.2011.05.044.

Turner, J.R., 2009. Intestinal mucosal barrier function in health and disease. Nat. Rev. Immunol. 9, 799–809. https://doi.org/10.1038/nri2653.

Wang, H.W., et al., 2017. Fluoride-induced oxidative stress and apoptosis are involved in the reducing of oocytes development potential in mice. Chemosphere 186, 911–918. https://doi.org/10.1016/j.chemosphere.2017.08.068.

Wang, H.W., et al., 2020. Fluoride-induced rectal barrier damage and microflora disorder in mice. Environ. Sci. Pollut. Res Int 27, 7596–7607. https://doi.org/10.1007/s11356-019-07201-8.

Yu, Y.M., et al., 2021. Estrogen deficiency aggravates fluoride-induced liver damage and lipid metabolism disorder in rats. Biol. Trace Elem. Res. https://doi.org/10.1007/s12011-021-02857-1.

Zhao, Y., et al., 2021. Exposed to mercury-induced oxidative stress, changes of intestinal microflora, and association between them in mice. Biol. Trace Elem. Res 199, 1900–1907. https://doi.org/10.1007/s12011-020-02300-x.

Zhou, B.H., et al., 2020. Drp1/Mff signaling pathway is involved in fluoride-induced abnormal fission of hepatocyte mitochondria in mice. Sci. Total Environ. 725, 138192 https://doi.org/10.1016/j.scitotenv.2020.138192.

Zhu, S.Q., et al., 2022. Fluoride exposure cause colon microbiota dysbiosis by destroyed microenvironment and disturbed antimicrobial peptides expression in colon. Environ. Pollut. 292, 118381 https://doi.org/10.1016/j.envpol.2021.118381.